



HAL
open science

Mobility of organic compounds in a soft clay-rich rock (Tégulines clay, France)

Ning Guo, Zoé Disdier, Emilie Thory, Jean-Charles Robinet, Romain Dagnelie

► **To cite this version:**

Ning Guo, Zoé Disdier, Emilie Thory, Jean-Charles Robinet, Romain Dagnelie. Mobility of organic compounds in a soft clay-rich rock (Tégulines clay, France). *Chemosphere*, 2021, 275, pp.130048. 10.1016/j.chemosphere.2021.130048 . cea-03540711v1

HAL Id: cea-03540711

<https://cea.hal.science/cea-03540711v1>

Submitted on 10 Mar 2023 (v1), last revised 10 Oct 2023 (v2)

HAL is a multi-disciplinary open access archive for the deposit and dissemination of scientific research documents, whether they are published or not. The documents may come from teaching and research institutions in France or abroad, or from public or private research centers.

L'archive ouverte pluridisciplinaire **HAL**, est destinée au dépôt et à la diffusion de documents scientifiques de niveau recherche, publiés ou non, émanant des établissements d'enseignement et de recherche français ou étrangers, des laboratoires publics ou privés.



Distributed under a Creative Commons Attribution - NonCommercial 4.0 International License

1
2
3
4
5
6
7
8
9
10
11
12
13
14
15
16
17
18
19
20
21
22
23

**Mobility of organic compounds in a soft clay-rich rock
(Tégulines clay, France)**

Ning Guo ^a, Zoé Disdier ^a, Émilie Thory ^a,
Jean-Charles Robinet ^b, Romain V.H. Dagnelie ^{a, *}

(a) Université Paris-Saclay, CEA, Service d'Étude du Comportement des Radionucléides, 91191, Gif-sur-Yvette, France

(b) Andra, R&D Division, parc de la Croix Blanche, 92298, Châtenay-Malabry, France

* Corresponding author. Université Paris-Saclay, CEA/DES/ISAS/DPC/SECR/L3MR, 91191, Gif-sur-Yvette, France.

E-mail address: romain.dagnelie@cea.fr

1 **Abstract**

2 The migration of organic compounds in soils is a major concern in several environmental
3 issues. Contaminants display distinct behaviours as regards to their specific affinities towards
4 soils constituents. The retention mechanism of hydrophobic compounds by natural organic
5 matter is well known. The retention of ionizable compounds is mainly related to oxides and
6 clay minerals, even if less documented in reductive media. In this work, we investigated the
7 migration of organic compounds in a soft clay-rich sedimentary rock (Tégulines clay, France).
8 The aim was to determine the relative contributions of natural sorbents on retention, and
9 eventual correlations with solutes properties. Both hydrophobic compounds (toluene,
10 benzene, naphthalene) and hydrophilic species (adipate, oxalate, ortho-phthalate, benzoate)
11 were investigated, using batch and diffusion experiments.

12 The retention of neutral aromatic compounds correlates with their lipophilicity ($\log P_{ow}$),
13 confirming that absorption mechanism prevails, despite a low content of natural organic
14 matter ($\leq 0.5\%$). A low retention of ionizable compounds was quantified on Tégulines clay.
15 The eventual discrepancies between data acquired on crushed rock and solid samples are
16 discussed. Low effective diffusion coefficients are quantified. These values hint on the
17 relative contributions of steric and electrostatic exclusion, despite a large pore size in such
18 “soft” clay-rock. Overall, the dataset illustrates a general scheme for assessing the migration
19 over a wide variety of organic compounds. This approach may be useful for predictive
20 modelling of the fate of organic compounds in environmental media.

21

22 **Keywords:**

23

24 Clay rock, Organic compound, Adsorption, Absorption, Diffusion, Anion exclusion

25

26 **Abbreviations and notations:**

27 α : Apparent porosity, accessible during diffusion of reactive solutes

28 ε : Porosity of media, accessible during diffusion of inert solutes, e.g. H₂O

29 Π : Exclusion factor from porous media quantified during diffusion

30 CO_x: Callovian-Oxfordian (Clay rock)

31 D_0 : Diffusion coefficient (m² s⁻¹) in water

32 D_e : Effective diffusion coefficient (m² s⁻¹) in porous media

33 f_{OM} / f_{CM} : Massic fraction of organic matter / clay minerals in sorbents

34 HDO: Semi-heavy water

35 IS: Ionic strength

36 K_{CM} : Contribution of clay minerals to the solid-liquid distribution coefficient (L kg(clay)⁻¹)

37 K_{OC} : Contribution of organic matter to the solid-liquid distribution coefficient (L kg(NOM)⁻¹)

38 NOM: natural organic matter

39 OPA: Opalinus (clay rock)

40 Orga: Organic (compound / sorbate)

41 P_{APP} : Apparent octanol water partition coefficient

42 P_{OW} : Octanol water partition coefficient (analogue to K_{ow})

43 R_d : Solid-liquid distribution coefficient (L kg⁻¹)

44 **1. Introduction**

45 The transport of organic compounds in environmental media is studied for various
46 applications: extraction of fossil fuels, fate of emerging organic contaminants, waste disposal
47 and remediation of soils. The term “organic” may be misleading, as it corresponds to a large
48 diversity of compounds: small ionizable compounds such as amino-acids, hydrophobic or
49 hydrophilic hydrocarbons, large synthetic or natural geopolymers and natural organic matter
50 (NOM) such as fulvic and humic acids. This work focuses on the transport of small soluble
51 molecules in the near surface of geological systems. Both ionizable carboxylic acids and
52 neutral aromatic compounds are investigated. The migration of such solutes in sedimentary
53 rocks is highly sensitive to sorption leading to diffusive retardation (Altmann et al., 2012;
54 Shackelford and Moore, 2013). Sorption-influenced transport is largely described in literature
55 for organic compounds (Borisover and Davis, 2015; Schaffer and Licha, 2015) indicating that
56 the retention part may originate from various mechanisms. Hydrophobic compounds, such as
57 alkanes and aromatic compounds are mainly absorbed by NOM (Borisover and Graber, 1997;
58 Karickhoff, 1981) with Freundlich-type sorption isotherm, eventually leading to intra-
59 particulate slow diffusion mechanism (Pignatello and Xing, 1996). On contrary, hydrophilic
60 compounds such as ionizable molecules are adsorbed on the surfaces of minerals, e.g. clays
61 and oxides (Gu et al., 1994; Hwang et al., 2007; Johnson et al., 2004; Kang and Xing, 2007).
62 Adsorption may be assumed in this case, with instantaneous and reversible Langmuir-type
63 isotherms, leading to increased apparent porosity and diffusive retardation factor. Both
64 mechanisms of adsorption and absorption, may occur simultaneously on the various
65 mineralogical components of a natural medium, but the relative contribution of these
66 mechanisms is rarely discussed.

67

68 Clay rock geological formations are considered in several countries for hosting a
69 radioactive waste disposal, e.g. Callovian-Oxfordian (COx) and Tégulines in France,
70 Opalinus Clay (OPA) and Helvetic Marl in Switzerland, Boom Clay in Belgium, etc.
71 (Altmann et al., 2012; Appelo et al., 2010; Maes et al., 2011). The COx clay rock has been
72 extensively studied in the context of the French Geological Radioactive Waste Disposal
73 (Cigéo project). Corresponding studies investigated the interaction between inorganic or
74 organic solutes and COx clay rock (Descostes et al., 2008; Melkior et al., 2007;
75 Rasamimanana, 2017a; Savoye et al., 2012). Absorption of neutral hydrophobic compounds
76 occurs in NOM (Vinsot et al., 2017), with an eventual contribution from clay minerals
77 (Willemsen et al., 2019). Similarly, the adsorption of organic anions occurs on clayey
78 minerals, despite a positive charge on clayey mineral surfaces (Rasamimanana et al., 2017b).
79 Still, electrostatic interactions between mineral surfaces and solutes leads to a partial
80 exclusion of anions from rock porosity. This so-called “anion exclusion” decreases both
81 effective diffusion coefficient and retardation factor of anions, as compared to neutral solutes
82 (Chen et al., 2018; Dagnelie et al., 2018). However, some major discrepancies are observed
83 between data measured by sorption on crushed clay rock and retardation factor observed in
84 solid samples. For that reason, the quantification of diffusive retardation factors seems
85 mandatory.

86

87 This work focuses on the Tégulines clay, from the Albian Gault geological formation
88 (East Paris Basin, France) under investigation for a potential near surface geological
89 radioactive waste repository (Lerouge et al., 2018; Missana et al., 2017). This repository
90 would confine low-activity long-lived waste, such as ^{14}C -graphite, remain from old natural
91 uranium graphite gas nuclear power reactor, developed in France until the 90s. In absence of
92 exhaustive characterization, the organic source term potentially released by radiolytic

93 lixiviation of graphite waste makes both neutral and anionic reference compounds being of
94 interest (Andra, 2015; Pageot et al., 2016, 2018; Poncet and Petit, 2013). The purpose of this
95 work is to quantify sorption and retardation factors of various organic species, in order to
96 assess the confinement properties of the geological barrier toward potential release of ^{14}C
97 bearing compounds. To that aim, diffusion experiments were performed and compared to
98 sorption experiments or predictive model based on media mineralogy. Moreover, the
99 comparison between results on Tégulines “soft” clay rock and COx “hard” clay rocks,
100 displaying variable compaction, are interesting to assess potential porosity exclusion and
101 effects on sorption-influenced transport of anions.

102

103 **2. Material and methods**

104 **2.1. Rock samples**

105 Experiments were carried out on Tégulines clay samples from the Albian Gault clay
106 formation. Rock samples were collected from two boreholes (AUB01918, AUB01825). The
107 cores were drilled at depths -20 and -22 m from the surface of the studied area (NE-SW) in
108 the eastern part of the Paris Basin (France) (Amédéo et al., 2017; Lerouge et al., 2018 and
109 2020). The mineralogical composition is detailed in supplementary data (Table S1). It is
110 basically composed of 50% of clay minerals, 40% of quartz, less than 5% of calcite and 0.6%
111 of NOM. After drilling, the core samples were protected from oxygen using container with
112 $\text{N}_{2(\text{g})}$. They were manipulated inside a glovebox ($P_{\text{O}_2}/P_0 < 2$ ppm) to prevent mineral
113 oxidation. The hydrated and “pasty” outlayer of the core was firstly removed and the inner
114 sound part of the rock was kept. The inner core was then sliced using a wire saw into disk
115 samples with a thickness of ~ 10 mm, and a diameter of ~ 35 -40 mm. The metrology of the
116 samples used in diffusion cells are provided in supplementary data (Table S2). These
117 measurements indicate an average hydrated density $\sim 1.98 \pm 0.10$ g cm^{-3} . The difference

118 between this hydrated density and clay rock dry density $\rho^{\text{dry}} \sim 1.7 \text{ g cm}^{-3}$ provides a rough
119 estimation of rock porosity: $\varepsilon = 28 \pm 10\%$. This value is in agreement with the results
120 obtained from diffusion experiments detailed subsequently. Some of the remaining off-cut
121 were crushed and sieved entirely below $125 \mu\text{m}$ for batch experiments.

122

123 A synthetic pore water was prepared by dissolution of pure salts (purity $> 99.5\%$) to
124 reach the composition for underground pore water of Gault formation clay rock (Ionic
125 strength: $\text{IS} = 2.33 \cdot 10^{-2} \text{ M}$, equilibrated $\text{pH} = 7.2 \pm 0.2$, Table S3). The synthetic water was
126 bubbled (1 L min^{-1}) with a mix of N_2/CO_2 (99/1) for more than 2 hours, removing O_2 and
127 equilibrating both dissolved CO_2 . The synthetic pore water was then mixed with “sacrificial”
128 crushed clay rock with a solid to liquid ratio of 10 g L^{-1} and agitated for more than 48 h. This
129 step was used for the equilibration of trace elements such as Fe, Al, Mn, Si and NOM.
130 Equilibrated pore water was filtrated through a $0.8 \mu\text{m}$ membrane to remove the sacrificial
131 clay. Additional filtration step through a $0.22 \mu\text{m}$ membrane was processed before
132 experiments to prevent bacterial activity. The composition of the equilibrated synthetic water
133 was analysed by ionic chromatography (Metrohm, 850 IC). Alkalinity was measured by
134 acidic dosage (HCOOH) in presence of methylene blue (Sarazin et al., 1999) with a UV-vis
135 spectrophotometer (Cary-500 from Agilent). The prepared pore water was used for pre-
136 equilibration step of clay samples, as described in the following section.

137

138 **2.2. Adsorption experiments**

139 The crushed clay ($< 125 \mu\text{m}$) was equilibrated for more than 48 hours with synthetic
140 pore water in sealed polycarbonate centrifugation tubes, with a solid to liquid ratio of 250 g
141 L^{-1} (1.5 g in 6 mL). Each tube was then spiked with ^{14}C or ^3H -organic tracer and agitated in a
142 shaking machine for 24 h at least, and up to 7 days. At the time of sampling, the tubes were

143 centrifuged over 50,000 g for 1 h and a fraction of the supernatant was sampled. The tracer
144 activity was determined by liquid scintillation counting on 1 mL samples (Packard TRICARB
145 2500), after addition of 4 mL of liquid scintillation solution (ultima goldTM cocktail). The
146 mass balance was checked for each tracer by duplicate experiments, i.e. without clay. The
147 variation of blank activity was below measurement accuracy ($\Delta A_0 < 2 \%$). All organic
148 molecules studied in this work and their properties are displayed in Table 1. Aromatic and
149 small carboxylic acids were chosen as compounds potentially released by degradation of
150 graphite. The compounds were also chosen in order to cover a wide range of lipophilicity (-4
151 $< \log D < 3.5$). The equilibrium concentration range was limited by the solubility of the
152 organic compound in aqueous solution and the specific activity of radioactive sources. When
153 available, full sorption isotherms cover a wide range of concentrations, thus providing
154 information on sorption process, e.g. isotherm shape and saturation of sorption sites
155 (Langmuir, Freundlich, etc.).

156

157 **Table 1** Properties of organic molecules. P_{OW} is the octanol water partition coefficient of carboxylic acids (RCOOH). $\log P_{APP}$ is the apparent
 158 partition coefficient in Tégulines pore water (pH ~ 7.2). $*pH^{EXP.} = 7.7 \pm 0.2$. Recommended values are in bold. $^{\$}$ Structure of molecules detailed
 159 in

160 S4.

Compound	Name (IUPAC)	Formula $^{\$}$	M _w (g mol ⁻¹)	pK _a ^[1]	Charge (pH 7.2)	log Pow ^[2,3,4]	log P _{APP} (Théor.)	log P _{APP} (Exp.)
o-phthalate	Benzene-1,2- dicarboxylic acid	C ₈ H ₆ O ₄	166.14	2.94, 5.43	Ph. ²⁻	0.73	-5.3	-2.77 ± 0.2*
Oxalate	Oxalic acid	C ₂ H ₂ O ₄	90.03	1.25, 4.14	Ox. ²⁻	-0.47	-9.5	-3.96 ± 0.2*

Table

[1]

161 (Haynes, 2014), [2] (Hansch et al., 1995), [3] (Pinsuwan et al., 1995), [4] (Sangster, 1989).

162	Benzoate	Benzoic acid	C ₇ H ₆ O ₂	122.12	4.20	Bz ⁻	1.87	-1.13	-1.26 ± 0.2*
	Adipate	Hexanedioic acid	C ₆ H ₁₀ O ₄	146.14	4.43, 5.42	Ad. ²⁻	0.08	-4.5	n.d.
	Naphthalene	Naphthalene	C ₁₀ H ₈	128.17	aprotic	N ⁰	3.32	3.4	3.3 ± 0.1
	Toluene	Toluene	C ₇ H ₈	92.14	aprotic	T ⁰	2.73	2.7	2.77 ± 0.1
	Benzene	Benzene	C ₆ H ₆	78.11	aprotic	B ⁰	2.13	2.1	1.82 ± 0.1

163 **2.3 Diffusion experiments**

164 Six diffusion experiments were conducted in typical through-diffusion cells
165 (numbering provided in Table 3), with a geometry detailed in Descostes et al., (2008) and
166 provided in Fig. S3. Prior to diffusion experiments, the rock samples were pre-equilibrated by
167 filling both upstream and downstream reservoirs with synthetic pore water. Clay was then
168 equilibrated more than 48h and solutions renewed several times in order to ensure chemical
169 equilibrium. Semi-heavy water (HDO) was used as a conservative reference, i.e. non sorbing
170 tracer with access to the whole porosity. To that aim, upstream solutions were spiked with
171 heavy water (D₂O). Both compartments were then periodically sampled. HDO content was
172 measured by infrared laser spectrometry (LGR, DLT-100 from Los Gatos Research). After
173 sampling, the upstream volume was refilled with initial injection solution and downstream
174 volumes refilled with raw pore water. After a few weeks of monitoring, upstream solution
175 was renewed by a solution with labelled organic tracers. The initial concentrations of organics
176 were controlled by Total Organic Carbon analysis (Vario TOC Cube from Elementar) for cold
177 solutions. Through-diffusion of organic compounds was monitored following the same
178 procedure than for HDO, except that samples were measured by liquid Scintillation Counter
179 (Packard TRICARB 2500 with ultima goldTM, Perkin Elmer).

180

181 2.4 Data modelling

182 Distribution between liquid and solid may follow two mechanisms: absorption or
183 adsorption. Absorption is a process in which an absorbate (atoms, molecules or ions) goes
184 into a bulk phase of absorbent. The mechanism at the interface can be considered as a
185 partitioning in two immiscible phases. Adsorption is a surface phenomenon, with an “increase
186 in the concentration of a substance at the interface between a condensed material (sorbent)
187 and in our case a liquid phase. Both absorption and adsorption can be quantified by a solid-
188 liquid distribution coefficient, R_d ($L\ kg^{-1}$):

189

$$R_d = \frac{q_e}{C_e} \quad (1)$$

190 where q_e ($mol\ kg^{-1}$) is the concentration of sorbed species per mass of sorbent, and C_e (mol
191 L^{-1}) the concentration in solution at equilibrium with the solid. In this work, the solid-liquid
192 distribution coefficient R_d ($L\ kg^{-1}$) is calculated using the following Eq. (2):

193

$$R_d = \left(\frac{C_0}{C_{eq}} - 1 \right) \times \frac{V}{m} = \left(\frac{A_0}{A_{eq}} - 1 \right) \times \frac{V}{m} \quad (2)$$

194

195 with C_0/C_{eq} ($mol\ L^{-1}$) being the initial/equilibrium concentrations in solution; A (Bq) the
196 activity, assumed proportional to C at any time; V (mL) the solution volume; and m (g) the
197 dry mass of clay rock. The uncertainty (u) on R_d values is calculated using uncertainties on
198 previous parameters through the Eq. (3):

199

$$u_{R_d}^2 = \left(\frac{V}{m \times A_{eq}} \right)^2 u_{A_0}^2 + \left(-\frac{A_0 V}{A_{eq}^2 m} \right)^2 u_{A_{eq}}^2 + \left(\frac{R_d}{V} \right)^2 u_V^2 + \left(\frac{R_d}{m} \right)^2 u_m^2 \quad (3)$$

200

201 Sorption isotherms can be described by several empirical equations. For example,
 202 Langmuir and Freundlich isotherms are described by Eq. (4) and Eq. (5), respectively, with
 203 K_L ($L \text{ mol}^{-1}$), K_F ($L^{(1/n)} \text{ kg}^{-1} \text{ mol}^{(1-1/n)}$), the affinity constants, and Q (mol kg^{-1}) the maximum
 204 sorbed amount. Langmuir-type isotherm is usually observed when adsorption occurs with a
 205 single energy interaction, leading to surface monolayers. Such behavior was evidenced by
 206 adsorption of hydrophilic organic molecules on COx clay rock (Rasamimanana et al., 2017a).
 207 Freundlich isotherm is more common when several interactions occur, e.g. including
 208 multilayer or absorption processes. The parameter $1/n$ can be seen as a sorption intensity
 209 (Karnitz et al., 2007). When $n = 1$, the Freundlich isotherm, Eq. (5), becomes analogue to
 210 partitioning, $R_d = K_F = C_{\text{org}}/C_{\text{eq}}$. In this work, Eq. (4) and Eq. (5) are respectively applied to
 211 describe the adsorption of hydrophilic organic molecules and absorption of lipophilic organic
 212 molecules in Tégulines clay rock.

213

$$q_e = Q \times \frac{K_L \times C_e}{1 + K_L \times C_e} \quad (4)$$

$$q_e = K_F \times C_e^{1/n} \quad (5)$$

214

215 The one dimensional analysis of diffusion results is based on Fick's second law
 216 (Crank, 1975), described by Eq. (6):

$$\frac{\partial C}{\partial t} = \frac{D_e}{\varepsilon_a + \rho(1-\varepsilon)R_d} \frac{\partial^2 C}{\partial x^2} = \frac{D_e}{\alpha} \frac{\partial^2 C}{\partial x^2} \quad (6)$$

217

218 with C represents the tracer concentration (mol L^{-1}), t the time (s), D_e the effective diffusion
 219 coefficient ($\text{m}^2 \text{ s}^{-1}$), ε and ε_a are the total and diffusion accessible porosities, ρ is the grain
 220 density of Tégulines clay rock ($\sim 1.7 \text{ kg L}^{-1}$), $\alpha = R \times \varepsilon$ is called the rock capacity factor. The
 221 normalized flux of tracer, J^{NORM} ($\text{m}^2 \text{ s}^{-1}$) is defined by Eq. (7):

222

$$J_{down}^{NORM}(t) = \frac{L}{C_0} \frac{dn_{down}(t)}{S \times dt} \quad (7)$$

223

224 where dn_{down} is the quantity of tracer reaching the downstream reservoir (moles), per unit of
225 time dt (s), and per sample surface S (m^2), L (m) the thickness of sample, and C_0 (moles m^{-3})
226 the initial upstream concentration.

227 The effective diffusion coefficient (D_e) and the rock capacity factor (α) are adjusted by
228 least-square fitting of both downstream flux and depletion of the upstream concentration. The
229 mass balance was assessed by comparison between upstream experimental data and
230 modelling. Satisfactory mass balances, $\Delta C \ll 5\%$, were obtained for all experiments, except
231 for toluene (Cell n° 6) which is discussed furtherly. Data and modelling for the reference
232 tracer, HDO, are provided in Fig. S4. The average values of D_e and ε for HDO obtained from
233 the 6 samples are $D_e = (1.38 \pm 0.37) \times 10^{-10} m^2 s^{-1}$ and $\varepsilon = 0.41 \pm 0.06$.

234

235 3. Results

236 3.1. Sorption of organic compounds on Tégulines clay

237 The Fig. 1 shows the experimental sorption results on Tégulines clay rock. R_d values
238 of ionizable compounds are rather constant as a function of equilibrium concentration. The
239 corresponding average value, R_d^{EXP} , for each organic compound are gathered in Table 2.
240 Some compounds display significant affinities (i.e. $\rho \times R_d \gg \varepsilon$). For example, the value R_d
241 (oxalate) = $4.7 L kg^{-1}$ is one order of magnitude higher than that of benzoate.

242

243
244
245
246
247
248
249
250
251
252
253
254
255
256
257
258
259
260
261
262
263
264
265
266
267

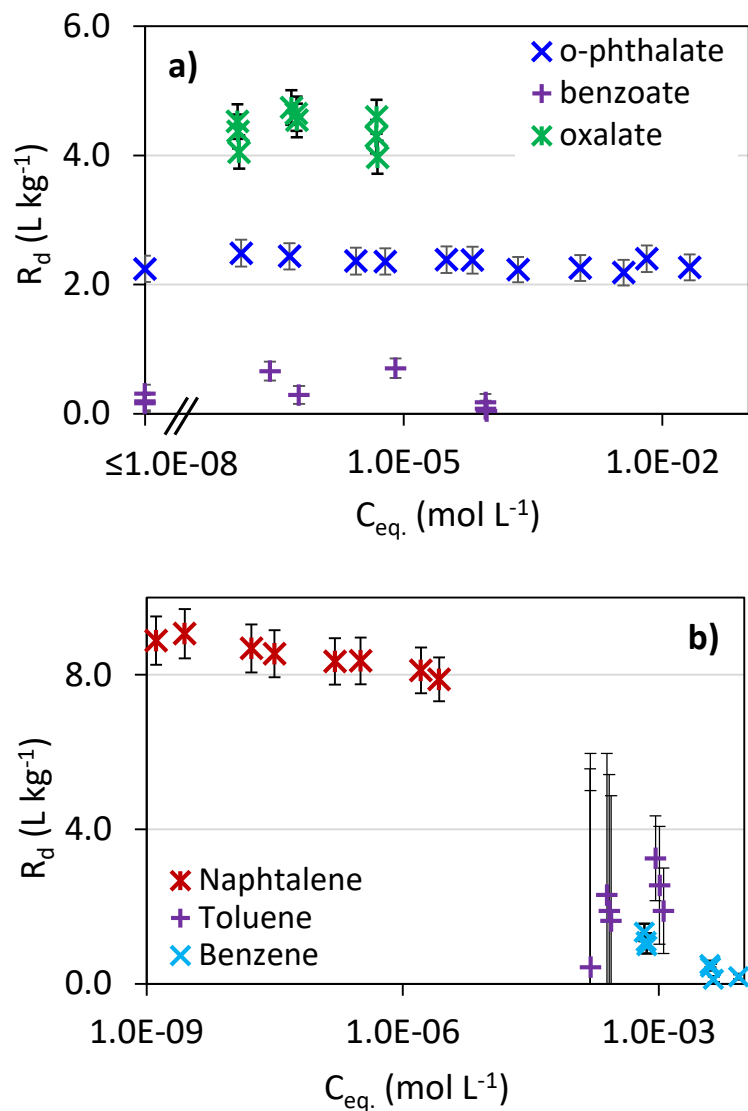


Fig. 1. Solid-liquid distribution coefficients (R_d) of organic compounds on Tégulines clay rock as a function of equilibrium concentration. $V/m = 4 \text{ L kg}^{-1}$, $\text{pH} = 7.2 \pm 0.2$, $T = 22 \pm 2^\circ\text{C}$.

(a) Data for ionizable compounds: o-phthalate, benzoate and oxalate.

(b) Data for neutral aromatic compounds: naphthalene, toluene and benzene.

The sorption isotherm of phthalate also displays a rather constant value. No clear saturation of sorption site is observed in the range of concentration measured, as expected in Langmuir-type shape (Eq. (4), Rasamimanana et al., 2017a). The best-fit modelling is provided in supplementary information (Fig. S2). Adjusted values are $Q = 1.5 \pm 2.1 \text{ mol kg}^{-1}$,

268 and $K_L = 1.6 \pm 2.2 \text{ L mol}^{-1}$, leading to $R_d^{\text{MAX}} \sim K_L \times Q = 2.3 \pm 4.5 \text{ L kg}^{-1}$. The o-phthalate
 269 compound displays higher affinity to Tégulines clay rock than benzoate. This highlights the
 270 role di-carboxylate group on sorption mechanism on the clay mineral surfaces
 271 (Rasamimanana et al., 2017a). Still, phthalate displays a weaker adsorption than oxalate,
 272 eventually linked to a steric effect, as discussed in Section 4.

273

274 **Table 2** Solid-liquid distribution coefficients measured by batch experiments on Tégulines
 275 clay rock. $\text{pH} = 7.2 \pm 0.2$, $T = 22 \pm 2 \text{ }^\circ\text{C}$. $V/m = 6 / 1.5 \text{ mL g}^{-1}$.

Compound	o-phthalate	Oxalate	benzoate	naphthalene	toluene	benzene
$R_d \text{ (L kg}^{-1}\text{)}$	2.33	4.65	0.55	9.10	2.57	1.14
$\pm u(R_d)$	± 0.10	± 0.10	± 0.23	± 0.23	± 0.68	± 0.18

276

277 The Fig. 1 also illustrate the sorption of neutral organic compounds on Tégulines clay
 278 rock. The R_d^{EXP} values of neutral organic compounds are displayed in Table 2, and exhibit
 279 with an order of naphthalene > toluene > benzene. The value $R_d \text{ (naphthalene)} = 9.1 \text{ L kg}^{-1}$, is
 280 one order of magnitude higher than that of benzene. These R_d values, from 1.14 to 9.10 L kg^{-1}
 281 are similar to that for ionizable compounds, despite rather different retention mechanism.
 282 Indeed, a slight decrease of R_d values is observed with the equilibrium concentration. Typical
 283 Freundlich isotherm, Eq. (5), was used to explain the naphthalene sorption isotherm, as
 284 illustrated in Fig. S2. The best fitting parameters are $K_F = 6.9 \pm 0.2$ and $n = 1.0$. The value of
 285 the constant $n = 1$ indicates a constant energy interaction and a sorption mechanism such as
 286 absorption (i.e. partitioning between two phases). The constant value of R_d in this range of
 287 concentration allows the use of similar equations for both ionizable and neutral compounds
 288 for modelling of diffusion experiments.

289

290

291 **3.2. Diffusion of organic compounds in Tégulines clay rock**

292 The results of through-diffusion experiments are illustrate in Fig. 2. A depletion of
293 upstream concentration and accumulation in downstream compartment (i.e. positive flux) is
294 observed with time increasing. Phthalate was observed in the downstream during the first day,
295 much earlier than adipate (~3 days) and oxalate (~15 days). This indicates a low retardation
296 factor and retention for o-phthalate. On contrary, toluene was detected in the downstream
297 after 14 days, indicating a higher retention. In the case of toluene, the non-linear sorption
298 isotherm leads to a slight deviation between observed and model data and an “apparent” bias
299 in mass balance. This does not affect significantly further estimation of the retardation factor,
300 based on the normalized flux. For other compounds, the model agreement between both
301 upstream and downstream data validates the model hypothesis, as well as mass balance of the
302 experiment.

303
304 For all compounds, a “steady state” is reached after a few tens of days, meaning a
305 constant flux of tracer. The normalized fluxes, calculated from downstream data with Eq. (7),
306 are shown in Fig. 2. The value of the plateau provides a visual estimation of effective
307 diffusion coefficients (D_e). The D_e of organic compounds in Tégulines clay rock ranges from
308 1 to $4 \times 10^{-11} \text{ m}^2 \text{ s}^{-1}$, with the order of phthalate < toluene < adipate < oxalate. These values
309 are one order of magnitude lower than the effective diffusion of HDO. The adjustment of
310 parameters D_e and α was performed using Eq. (7) by adjusting simultaneously both upstream
311 and downstream data. The corresponding best fit values of D_e and α values are gathered in
312 Table 3. The rock capacity factors ($\alpha = R \varepsilon$), sometimes referred as “apparent porosity”, range
313 from 0.47 (phthalate) to 7.72 (oxalate), higher than the total porosity quantified with HDO (ε
314 = 0.41). This data quantifies the retention of the molecules during migration in Tégulines clay

315 rock. The corresponding solid-liquid distribution ratios calculated from Eq. 6 are discussed in
316 the following sections.

317 **Table 3** Reference of diffusion cell experiments, n°1 to 6. Corresponding diffusion parameters adjusted from experimental results (HDO for
 318 water tracer). D_0 values are taken from Haynes (2014). *reprocessed to account for the experimental diffusion gradient.

319

Diffusion cell (Tracer)	IS (M)	D_e (water) ($10^{-10} \text{ m}^2 \text{ s}^{-1}$)	ε (water)	α (org)	D_0 (org) ($10^{-10} \text{ m}^2 \text{ s}^{-1}$)	D_e (org) ($10^{-12} \text{ m}^2 \text{ s}^{-1}$)	Π	R_d^{CELL} (L kg^{-1})	R_d^{BATCH} (L kg^{-1})
Cell n°1 ³H-phthalate	0.02	1.04 ± 0.05	0.41 ± 0.06	0.47 ± 0.05	6.96	10.05 ± 0.70	0.32 ± 0.03	0.16 ± 0.04	2.33 ± 0.10
Cell n°2 ³H-adipate	0.02	1.43 ± 0.16	0.45 ± 0.06	0.64 ± 0.10	6.39	23.63 ± 2.70	0.58 ± 0.10	0.30 ± 0.08	-
Cell n°3 ¹⁴C-oxalate	0.02	1.65 ± 0.21	0.47 ± 0.08	7.58 ± 1.50	9.87	36.44 ± 4.50	0.52 ± 0.10	5.93 ± 1.22	4.65 ± 0.10
Cell n°4 ¹⁴C-oxalate (phthalate)	0.32	0.96 ± 0.05	0.34 ± 0.05	5.59 ± 1.20	9.87	23.32 ± 4.70	0.57 ± 0.11	4.31 ± 0.97	-
Cell n°5 ¹⁴C-oxalate (NaNO_3)	0.32	1.93 ± 0.23	0.46 ± 0.06	11.12 ± 1.10	9.87	40.84 ± 2.80	0.50 ± 0.07	8.80 ± 0.89	-
Cell n°6 ³H-toluene	0.02	1.30 ± 0.04	0.41 ± 0.05	3.30 ± 0.80	8.50	38.7* ± 3.6	0.82 ± 0.8	2.45 ± 0.65	2.57 ± 0.68

320
321
322
323
324
325
326
327
328
329
330
331
332
333
334
335
336
337
338
339
340
341
342
343
344

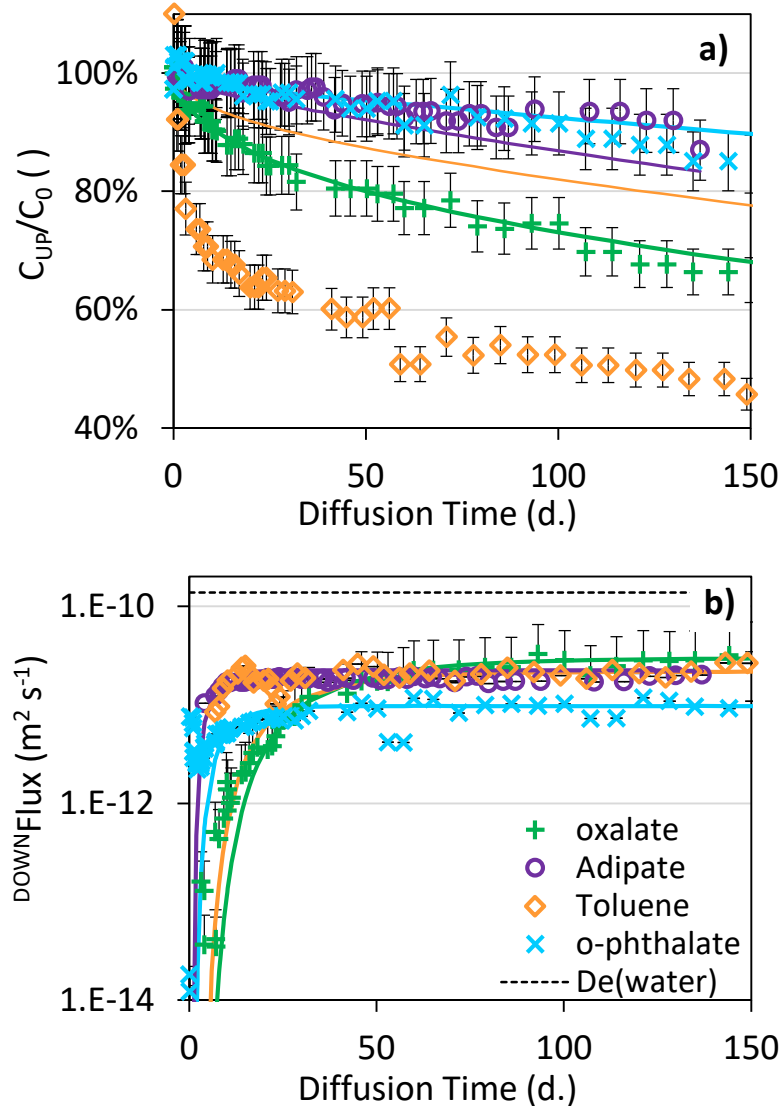


Fig. 2. Diffusion data of organic compounds in Tégulines clay rock.

(a) Upstream concentration (b) Normalized Downstream flux. Solid lines represent best fit modelling (Upstream and downstream data adjusted simultaneously). Dashed line represents the average value measured for water, $D_e(water) = (1.38 \pm 0.37) \times 10^{-10} m^2 s^{-1}$.

3.4. Co-diffusion of organic and inorganic solutes

In order to get insights on the various mechanism occurring, e.g. anion exclusion and synergetic or competitive effects, the diffusion of oxalate was measured in presence of

345 organic and inorganic plumes. Additional through-diffusion experiments were performed with
346 ionic strength increased by an order of magnitude, i.e. from $2.33 \cdot 10^{-2}$ M in Tégulines pore
347 water, up to $3.2 \cdot 10^{-1}$ M. Ionic strength (IS = 0.32 M) was imposed by the presence of 0.1 M
348 sodium phthalate and 0.3 M NaNO_3 respectively. Diffusion data of oxalate under these
349 conditions are provided in Fig. S6. The adjusted parameters, including D_e and α values,
350 are displayed in Table 3. Significant variation of $D_e(\text{oxalate})$ and $\alpha(\text{oxalate})$ values are
351 observed in presence of saline and organic plume. Yet, the difference between both
352 experiments, i.e. o-phthalate and NaNO_3 plume, indicates that ionic strength is not the only
353 parameter affecting migration and anion exclusion. The transitory state during diffusion of
354 oxalate lasted ~ 15 days in raw Tégulines pore water. This transitory state was shorter (10
355 days) in presence of 0.3 M NaNO_3 , while much longer (30 days) with addition of 0.1 M
356 sodium phthalate. Hence, both experiments at high ionic strengths induced opposite
357 disturbances compared to the “sound” state. These effects are quantified by the effective
358 diffusion coefficients, D_e , which is an indicator of charge or steric exclusion, and rock
359 capacity factor, α , which is an indicator of retention (Table 3). The possible mechanisms
360 occurring, e.g. anion exclusion or pH drift are reviewed in the following section.

361

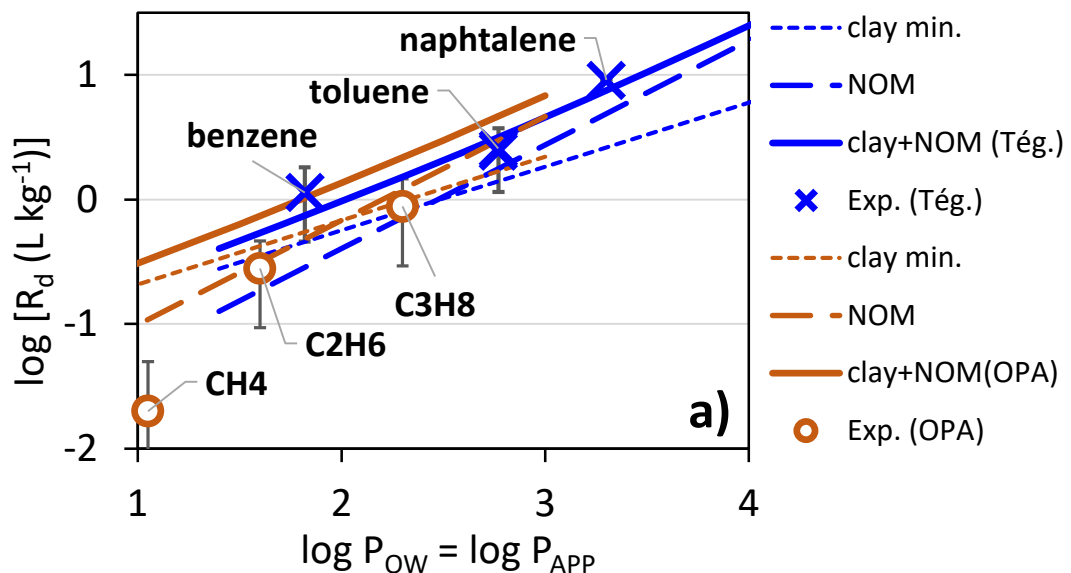
362

363 4. Discussion

364 4.1 Retention of lipophilic compounds ($\log P_{ow} > 1$)

365 The interaction between neutral aromatic compounds and soils is mainly related to
366 absorption mechanism into NOM. Such hypothesis is easily assessed by representing the
367 correlation between retention and lipophilicity of sorbates (Karickhoff et al., 1979).
368 Lipophilicity of solutes is usually quantified by their octanol/water partition coefficient, P_{ow} .
369 Strong correlations are observed between P_{ow} values and affinity on the NOM fraction of
370 sorbents, i.e. $K_{OC} = R_d/f_{OC}$ (f_{OC} being the mass fraction of organic matter in the sorbent). Such
371 correlation is illustrated in Fig. S7, with the corresponding linear regression $\log K_{OC} \sim 0.84 \times$
372 $\log P_{ow} + 0.23$ ($R^2 = 0.84$). The slope of the curve: +0.84 traduces a thermodynamic
373 equilibrium, with similar interactions involved in absorption and partitioning mechanisms,
374 e.g. free enthalpy of solvation. The value $\log K_{OC} = +1.07$ (for $\log P_{ow} = +1$) quantifies a
375 strength of interaction between slightly lipophilic solutes and NOM. On the other hand, the
376 affinity between clay minerals and organic solutes is also well documented (Barré et al.,
377 2014) and similar correlations due to hydrophobic interactions are expected (Willemsen et al.,
378 2019). Yet, the correlations between retention and $\log P_{ow}$ are less obvious, as illustrated in
379 Fig. S7, with $\log K_{CM} \sim 0.51 \times \log P_{ow} - 0.98$. The low correlation ($R^2 = 0.11$) and strong
380 data disparity are caused by the diversity of phyllosilicates structures, as well as various
381 adsorption mechanisms (Barré et al., 2014). Still, the value $\log K_{CM} = -0.47$ (for $\log P_{ow} =$
382 $+1$) indicates an affinity of clay minerals, almost two orders of magnitude below the previous
383 value for NOM. Hence, the two previous correlations are useful to assess, in a first
384 macroscopic approach, the respective contributions of NOM and clay minerals to the retention
385 in sedimentary rocks. Fig. 3 (a) illustrates the relative contributions of absorption in NOM and
386 of adsorption on clay minerals in two examples of sedimentary rocks. The agreement between
387 predicted values and experimental data on Tégulines ($f_{OC} \sim 0.5\%$, $f_{CM} \sim 50\%$) and OPA ($f_{OC} \sim$

388 0.8%, $f_{CM} \sim 60\%$) clay rocks is rather good. The fact that clay minerals contribution displays a
 389 lower slope than NOM contribution induces interesting features. The contribution of
 390 absorption mechanism in NOM prevails for high values of $\log P_{OW}$. This remains true even in
 391 sedimentary rocks with low NOM content, such as Tégulines clay rock ($f_{OC} = 0.5\%$, Lerouge
 392 et al., 2018), OPA clay ($f_{OC} = 0.5\%$, Wersin et al., 2008), or COx clay rock ($f_{OC} = 0.6\%$,
 393 Gaucher et al., 2004). On the other hand, the adsorption on phyllosilicates may control the
 394 retention of solutes with low $\log P_{OW}$ values, especially for such rocks with high contents of
 395 clay minerals ($f_{CM} > 50\%$). As a corollary, the accurate measurement of low NOM content
 396 ($f_{OC} < 1\%$) provides a useful data, complementary to clay mineralogy. This allows to
 397 determine sorbing phases and predict the migration of lipophilic compounds (dissolved gas,
 398 pesticides, etc.) in sedimentary rocks and geobarriers.



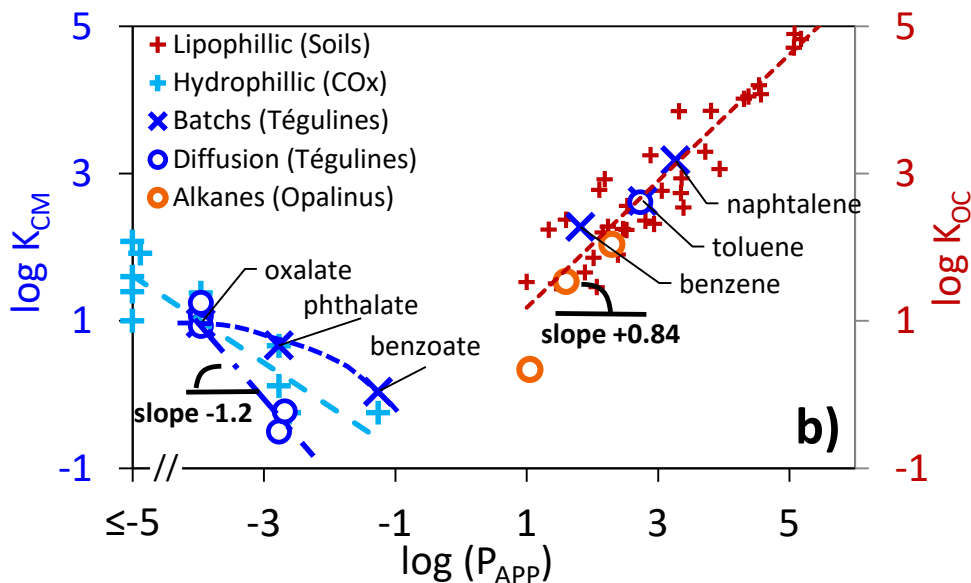


Fig. 3. Correlation between partition coefficient of organic compounds and their retention properties in natural media (near neutral pH ~ 7.2).

a) Data for lipophilic compounds ($\log P_{APP} > 1$) measured on Tégulines (Tég.) and Opalinus (OPA) clay rocks. Dashed lines: theoretical contribution expected from absorption in NOM and adsorption on phyllosilicates. Signs correspond to experimental data: Adsorption and through-diffusion in Tégulines at $22 \pm 2^\circ\text{C}$ (This work), In situ out-diffusion experiment in OPA at $16.5 \pm 1.5^\circ\text{C}$ (Vinsot *et al.*, 2017). b) Comparison of adsorption data for hydrophilic compounds ($K_{CM} = R_d/f_{CM}$) and absorption data of lipophilic compounds ($K_{OC} = R_d/f_{OC}$). Data on Tégulines (This work), OPA (Vinsot *et al.*, 2017), COx clay rock (Rasamimanana *et al.*, 2017a) and soils (Karickhoff *et al.*, 1981).

4.2 Retention of hydrophilic compounds ($\log P_{APP} < -1$)

Ionizable compounds are among the most widespread hydrophilic compounds. For carboxylates (RCOO^-), octanol/water apparent partition coefficient may be estimated from the value of carboxylic acids (RCOOH) using the Eq. 8 (Sangster, 1989):

$$P_{APP} = \frac{P_{OW}}{1 + 10^{(pH - pK_{a1})}} \quad (8)$$

437

438 However, such equation becomes unsuitable for highly hydrophilic compounds. For
 439 that reason, log P_{APP} values were experimentally measured in this study. The methodology
 440 and results are provided in supplementary material (Fig. S1). The corresponding values are
 441 gathered in Table 1. As for hydrophilic compounds, a correlation is observed between log R_d
 442 and log P_{APP} values of ionizable compounds (Fig. 3, b). In this case, the slope is negative,
 443 which indicates a retention mechanism differing from that for aromatic compounds, i.e. more
 444 likely an adsorption mechanism on surfaces of clayey minerals. Hence, R_d values are
 445 normalized by the content of clay minerals in the media, $K_{CM} = R_d/f_{CM}$, in order to ease the
 446 comparison between rocks. Results on Tégulines soft clay rock (Fig. 3, b) are in line with data
 447 previously published on COx hard clay rock (Chen et al., 2018; Durce et al., 2015;
 448 Rasamimanana et al., 2017b). A linear correlation is observed between retention of solutes
 449 and hydrophilicity of sorbates and that solvation and retention mechanism involve similar
 450 interactions. Moreover, the value of the slope close to unity, (-1.2 ± 0.1) , tends to indicate that
 451 thermodynamic equilibrium is reached during diffusion experiments. Some correlation
 452 between hydrophilicity of ionizable sorbates and retention has been previously reported on
 453 COx clay rock, but without evidence of any sorption “maximum” (Rasamimanana et al.,
 454 2017a). The correlation observed on Tégulines clay rock, $K_{CM} = f(\log P_{APP})$, seems to point
 455 out a rise to a plateau for highly hydrophilic sorbates, e.g. oxalate. This means that below a
 456 certain value of log P_{APP} , the affinity between hydrophilic sorbates and minerals does not
 457 increase “indefinitely”. This trend differs from the affinity of lipophilic compounds which
 458 increases up to log P_{OW} values over +6.

459 Speciation calculation are illustrated in supplementary material (Fig. S8). Data
 460 indicates that the acidic form of solutes becomes negligible at near-neutral pH. Hence, the

461 retention mechanism may imply anionic species, rather than protonated organic acids. On the
462 other hand, the relative contribution of mineralogical phases (especially clay minerals and
463 oxides) to the retention of ionizable compounds deserves further numerical or experimental
464 investigations (Ilina et al., 2020). For example, the presence of oxidized minerals in samples
465 may contribute to differences between batch and diffusion experiments, as observed for o-
466 phthalate and discussed furtherly.

467

468 **4.3. Diffusion data and exclusion from rock porosity**

469 The effective coefficients obtained from the diffusion experiments are lower than that
470 of water, almost by an order of magnitude (Table 3). This behaviour is usually explained by a
471 phenomenon of anion exclusion in surface charged media (de Haan, 1968). Such data can be
472 discussed using the exclusion factor, Π , defined by Eq. 9:

473

$$\Pi(\text{solute}) = \frac{D_e(\text{solute})/D_e(\text{water})}{D_0(\text{solute})/D_0(\text{water})} \quad (9)$$

474

475 where D_e is the effective diffusion coefficient in the porous solid and D_0 in water. The ratio
476 $D_e(\text{solute})/D_e(\text{water})$ quantifies the effect of clay rock on the diffusion of a solute, in
477 comparison with non-reactive species such as water. This ratio is then normalized by
478 $D_0(\text{solute})/D_0(\text{water})$, in order to remove the contribution of solvent (poral water) on the
479 diffusivity. Thus, the exclusion factor Π isolates the effect from the porosity of the media (i.e.
480 tortuosity and constrictivity, Van Brakel and Heertjes, 1974) on the diffusion pathways of
481 solutes. Fig. 4 shows the exclusion factor of anionic solutes as a function of their sizes
482 (estimated from molecular mass). Data is reported for both COx and Tégulines clay rocks.
483 Previous studies evidenced anion exclusion in COx clay rock for both inorganic (Descostes et
484 al., 2008) and organic anions (Dagnelie et al., 2018), with exclusion factors down to 0.1 (i.e.
485 $\Pi(\text{anion}) \ll \Pi(\text{water}) = 1$). This phenomena is usually explained by the presence of surface

486 charged clay minerals (Tournassat et al., 2016) and more pronounced when pore size is small
487 (Gaboreau, et al., 2016; Wigger et al., 2018). For example, a strong anion exclusion is
488 observed in COx clay units (UA2, UA3, <-450 m in depth), quantified with $\Pi(\text{Cl}^-/\text{COx}) \sim 0.3$
489 ± 0.1 (Descostes et al., 2008). In contrast, no anion exclusion was evidenced with chloride in
490 Tégulines soft clay rock, despite similar content in clay minerals. The absence of chloride
491 exclusion in Tégulines, $\Pi(\text{Cl}^-/\text{Tégulines}) \sim 1$, can be explained by the shallow depth of the
492 media: -75 m to -10 m (Debure et al., 2018). This leads to a less dense material ($\rho^{\text{dry}} \sim 1.7 \text{ g}$
493 cm^{-3}), and a limited diagenetic processes with pore diameters mainly higher than 30–50 nm
494 (Lerouge et al., 2018).

495 Surprisingly, a significant exclusion was observed for organic molecules in Tégulines
496 clay rock, thus differing from chloride case (Fig. 4, a). Regarding exclusion from porosity, the
497 size of diffusing solutes may also decrease exclusion factor by steric effect, as clearly
498 evidenced with neutral species, $\Pi(\text{toluene}/\text{Tégulines}) \sim 0.82 \pm 0.08$. The values for adipate
499 and oxalate, $\Pi \sim 0.5 \pm 0.1$, are even lower than that of toluene (despite similar mass),
500 indicating an additional contribution of charge to the exclusion from porosity. Still, the value
501 of $\Pi(\text{organic anions})$ mainly decreases with the size of solutes (Fig. 4) for both Tégulines and
502 COx clay rock. These trends indicate that the exclusion factors of complex anions is highly
503 related to their sizes as compared to the size of pores in the media. Hard COx rock, with a
504 pore size $\sim 6\text{-}8 \text{ nm}$, displays a strong anion exclusion, even for chloride. Only small inorganic
505 anion, such as Cl^- , display little exclusion factor in soft Tégulines rock (pore size $\sim 20\text{-}30$
506 nm). Since a significant exclusion is observed for larger species in both soft and hard rocks,
507 other anions than Cl^- should be preferred to quantify exclusion factor of environmental media,
508 e.g. NO_3^- SO_4^{2-} . These references, if conservative in the media, should be more representative
509 of other contaminants such as AsO_4^{3-} or SeO_4^{2-} .

510
 511
 512
 513
 514
 515
 516
 517
 518
 519
 520
 521
 522
 523
 524
 525
 526
 527
 528
 529
 530
 531
 532
 533

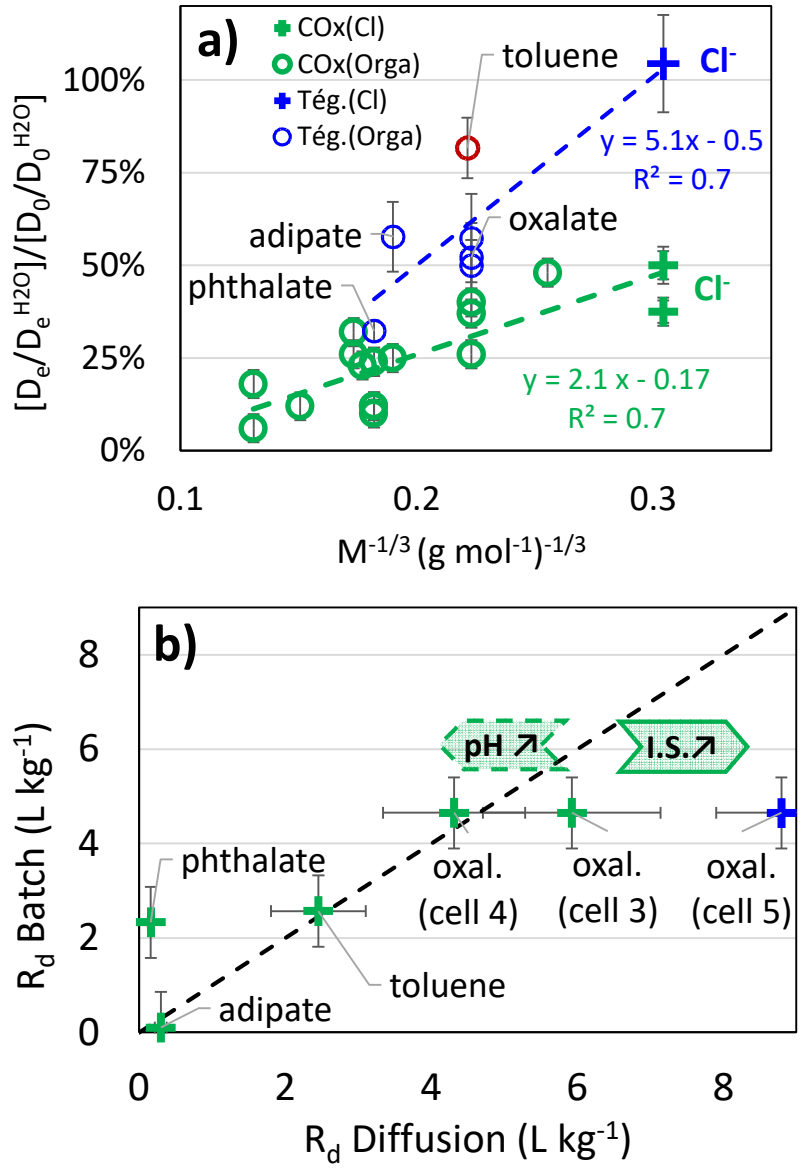


Fig. 4. Diffusion data for organic solutes. a) Exclusion factor for organic anions in COx clay rock (Dagnelie et al., 2014, 2018) and in Tégulines clay rock (Tég.) (This work). M: molecular mass. b) Solid-liquid distribution coefficient, R_d ($L\ kg^{-1}$), measured in Tégulines by batch experiments (X axis) and diffusion experiments (Y axis).

534 **4.4. Retardation and environmental implications**

535 Assessing the environmental impact of hazardous materials requires the estimation of
536 their migration properties, such as sorption, retardation and diffusivity. The predictive
537 migration modelling in natural media requires several building blocks. This includes accurate
538 description of the media, sorbing phases, and understanding of retention processes. It is then
539 useful to assess retention by various methodologies, e.g. molecular simulations, batch
540 experiments, migration experiments. This approach strengthen the description on underlying
541 phenomena and the accuracy on corresponding data. Such comparison of results is provided
542 in Fig. 4 (b). A large discrepancy is quantified between batch and diffusion data for slightly
543 lipophilic compounds, i.e. $-4 < \log P_{APP} < 0$, similarly to previous data on COx clay rock
544 (Dagnelie et al., 2018) or compacted clay minerals (Chen et al., 2018). This discrepancy is
545 especially striking for o-phthalate, for which diffusion data suggests strong steric and charge
546 exclusion. Similar observations on COx clay rock and illite suggest a “collapse” of retardation
547 when exclusion factor decreases below a “threshold” value. Yet, the mechanism leading to
548 such discrepancy is unclear. Further investigations are required to assess eventual hypotheses,
549 e.g. effect of anion exclusion on surface accessibility, oxidative perturbation of sulphide
550 minerals in crushed samples leading to additional (hydroxy)oxides, kinetic effects, etc.
551 Meanwhile, diffusion experiments and especially long-term *in situ* experiments seem
552 mandatory in order to accurately quantify the retardation factor of such solutes.

553
554 The batch and diffusion experiments provided consistent data for both toluene (\log
555 $P_{APP} = 2.73$, lipophilic) and oxalate ($\log P_{APP} = -3.96$, hydrophilic). This validates the reactive
556 transport model, despite simplistic hypothesis (reversible and instantaneous retention) and the
557 absence of speciation calculations. The good agreement between results from both types of
558 experiments strengthens the accuracy on corresponding values: R_d (toluene/Tégulines) $\sim 2.5 \pm$

559 0.3 L kg⁻¹ and $R_d(\text{oxalate}/\text{Tégulines}) \sim 4.5 \pm 0.5 \text{ L kg}^{-1}$. Given the relatively good accuracy
560 on oxalate retention data, this later compounds was chosen for further co-diffusion
561 experiments. In the case of pollution events, the concomitant release of various contaminants
562 leads to co-sorption and co-diffusion phenomena. Several mechanisms may affect retention:
563 competitive sorption, pH drift, modification of IS, etc. In this context, diffusion of oxalate was
564 performed in presence of 0.1 M of o-phthalate (diffusion cell n°4) or 0.3 M of NaNO₃
565 (diffusion cell n°5). The retention of oxalate in sound sample (cell n°3), in presence of
566 phthalate (cell n°4), and in batch experiments, are in agreement with regard to the
567 uncertainties. This demonstrates that eventual pH drifts (between 7 and 9) due to the presence
568 of organic plume (Fralova et al., 2021) do not affect significantly diffusion. On contrary, a
569 slight increase of $R_d(\text{oxalate})$ is observed in presence of NaNO₃. This result may be linked to
570 the effect of ionic strength, which decreases anion exclusion, and thus increases accessibility
571 to surfaces and retardation. It is interesting to note that such an effect was not observed in cell
572 4, despite a similar ionic strength. This may probably be due to the diffusion speed of the
573 perturbation compared to oxalate diffusion. The effective diffusion coefficient of o-phthalate
574 is lower than that of oxalate. Thus in cell 4, the phtalate plume might diffuse too “slowly” to
575 affect significantly the diffusion of oxalate. Whereas in cell 5, the effective diffusion of NO₃⁻,
576 which is faster than oxalate (Dagnelie et al., 2017), leads to an increase of IS along the
577 pathway of oxalate. Such effect may be responsible of the decrease of anion exclusion and
578 eventual increase of retention. This also confirms that oxalate exclusion is partially induced
579 by charge effects (in addition to steric effects), which is in agreement with measured
580 exclusion factors (i.e. $\Pi(\text{oxalate}) < \Pi(\text{toluene})$, Fig. 4). Overall, these results illustrate the
581 various mechanisms, with eventual antagonist effects, which may arise from release of
582 complex saline and organic plumes during pollution events.

583

584

585 **Conclusion**

586 Retention and diffusion of various organic compounds were quantified in the
587 Tégulines soft clay rock. A comparison is made with previous data measured on COx hard
588 clay rock. A significant affinity with clay rich rocks was observed for both lipophilic ($\log P_{ow}$
589 > 1) and hydrophilic ($\log P_{APP} < -1$) compounds. Neutral aromatic compounds mainly
590 undergo absorption mechanism in NOM. Such absorption is well correlated with the content
591 of NOM in the sorbent and the lipophilicity of the sorbate. The organic phase remains the
592 main sorbent for such compounds, even in media with low organic content, $f_{OC} \leq 0.6\%$. Still,
593 clay minerals may contribute to the retention of low lipophilicity compounds in such clay-rich
594 rocks ($f_{CM} \geq 40\%$). Nevertheless, the retention measured on crushed clay rock accurately
595 predict retardation measured by diffusion experiments. Additional mechanism of
596 intraparticulate diffusion should eventually be taken into account for migration modelling.

597 The ionizable compounds displayed values of solid-liquid distribution coefficients
598 similar to neutral compounds, but caused to adsorption mechanism. Surprisingly, this
599 adsorption was also correlated with the lipophilicity of solutes, with a maximum affinity
600 reached when $\log P_{APP} \leq -4$. The diffusion data evidences an exclusion from rock porosity,
601 with a contribution of both size and charge of solutes. Such exclusion is higher for large
602 organic anions than for “small” inorganic anions such as chloride. The diffusive retardation of
603 solutes with intermediate polarities ($\log P_{APP} \sim -2$), such as o-phthalate, was lower than
604 expected from batch experiments. Further studies would be interesting in order to quantify the
605 relative contribution of clay minerals and (hydroxy)oxides on the retention mechanisms.

606

607 **Acknowledgments**

608 This work was financed by CEA and the French radioactive waste management agency
609 (Andra).

610

611 **References**

- 612 Altmann, S., Tournassat, C., Goutelard, F., Parneix, J.C., Gimmi, T., Maes, N., 2012. Diffusion-driven
613 transport in clayrock formations. *Appl. Geochemistry* 27, 463–478.
- 614 Andra, 2015. Projet de stockage des déchets radioactifs de faible activité massique à vie longue
615 (FAVL) – Rapport d'étape 2015. FRPADPG150010.
- 616 Amédéo, F., Matrimon, B., Deconinck, J.-F., Huret, E., Landrein, P., 2017. Les forages de Juzanvigny
617 (Aube, France): litho-biostratigraphie des formations du Barrémien à l'Albien moyen dans l'est du
618 bassin de Paris et datations par les ammonites. *Geodiversitas* 39, 185–212.
- 619 Appelo, C.A.J., Van Loon, L.R., Wersin, P. 2010. Multicomponent diffusion of a suite of tracers
620 (HTO, Cl, Br, I, Na, Sr, Cs) in a single sample of Opalinus Clay. *Geochim. Cosmochim. Acta* 74,
621 1201–1219.
- 622 Barré, P., Fernandez-Ugalde, O., Virto, I., Velde, B., Chenu, C. 2014. Impact of phyllosilicate
623 mineralogy on organic carbon stabilization in soils: incomplete knowledge and exciting prospects.
624 *Geoderma* 235–236, 382–395.
- 625 Borisover, M.D., Graber, E.R., 1997. Specific interactions of organic compounds with soil organic
626 carbon. *ACS Div. Environ. Chem. Prepr.* 37, 172–174.
- 627 Borisover, M., Davis, J.A., 2015. Adsorption of Inorganic and Organic Solutes by Clay Minerals. *Dev.*
628 *Clay Sci.* 6, 33–70.
- 629 Van Brakel, J., Heertjes. P.M., 1974. Analysis of Diffusion in Macroporous Media in Terms of a
630 Porosity, a Tortuosity and a Constrictivity Factor. *International Journal of Heat and Mass Transfer* 17
631 (9), 1093–1103.
- 632 Chen, Y., Glaus, M.A., Van Loon, L.R., Mäder. U., 2018. Transport of Low Molecular Weight
633 Organic Compounds in Compacted Illite and Kaolinite. *Chemosphere* 198, 226–37.
- 634 Crank, J. 1975. *The Mathematics of Diffusion*. London: Clarendon Press.
- 635 Dagnelie, R.V.H., Descostes, M., Pointeau, I., Klein, J., Grenut, B., Radwan, J., Lebeau, D., Georgin,
636 D., Giffaut, E., 2014. Sorption and diffusion of organic acids through clayrock: comparison with
637 inorganic anions. *J. Hydrol.* 511, 619–627.

638 Dagnelie, R.V.H., Arnoux, P., Enaux, J., Radwan, J., Nerfie, P., Page, J., Coelho, D., Robinet, J.-C.,
639 2017. Perturbation induced by a nitrate plume on diffusion of solutes in a large-scale clay rock sample.
640 *Appl. Clay Sci.* 141, 219–226.

641 Dagnelie, R.V.H., Rasamimanana, S., Blin, V., Radwan, J., Thory, E., Robinet, J.-C., Lefèvre, G.,
642 2018. Diffusion of Organic Anions in Clay-Rich Media: Retardation and Effect of Anion Exclusion.
643 *Chemosphere* 213, 472–80.

644 Debure, M., Tournassat, C., Lerouge, C., Madé, B., Robinet, J.-C., Fernández, A.M., Grangeon, S.,
645 2018. Retention of Arsenic, Chromium and Boron on an Outcropping Clay-Rich Rock Formation (the
646 Tégulines Clay, Eastern France). *Sci.Total Environ.* 642, 216–29.

647 Descostes, M., Blin, V., Bazer-Bachi, F., Meier, P., Grenut, B., Radwan, J., Schlegel, M.L.,
648 Buschaert, S., Coelho, D., Tevissen, E., 2008. Diffusion of Anionic Species in Callovo-Oxfordian
649 Argillites and Oxfordian Limestones (Meuse/Haute-Marne, France). *Appl. Geochem.* 23, 655–77.

650 Durce, D., Bruggeman, C., Maes, N., Van Ravestyn, L., Brabants, G. 2015. Partitioning of organic
651 matter in Boom Clay: Leachable vs mobile organic matter. *Appl. Geochem.* 63, 69–181.

652 Fralova, L., Lefèvre, G, Madé, B., Marsac, R., Thory, E., Dagnelie, R.V.H. Effect of organic
653 compounds on the retention of radionuclides in clay rocks: Mechanisms and specificities of Eu(III),
654 Th(IV), and U(VI). *Appl. Geochem.* 104859, 2021.

655 Gaboreau, S., Robinet, J.-C., Prêt, D. 2016. Optimization of Pore-Network Characterization of a
656 Compacted Clay Material by TEM and FIB/SEM Imaging. *Microporous and Mesoporous Mater.* 224,
657 116–128.

658 Gaucher, E., Robelin, C., Matray, J.-M., Négrel, G., Gros, Y., Heitz, J.F., Vinsot, A., Rebours, H.,
659 Cassagnabère, A., Bouchet, A., 2004. ANDRA underground research laboratory: interpretation of the
660 mineralogical and geochemical data acquired in the Callovian–Oxfordian formation by investigative
661 drilling. *Phys. Chem. Earth*, 29, 55–77.

662 Gu, B., Schmitt, J., Chen, Z., Liang, L., McCarthy, J.F., 1994. Adsorption and Desorption of Natural
663 Organic Matter on Iron Oxide: Mechanisms and Models. *Environ. Sci. Technol.* 28, 38–46.

664 de Haan, F.A.M., 1968. The Negative Adsorption of Anions (Anion Exclusion) in Systems with
665 Interacting Double Layers. *J. Phys. Chem.* 68 (10), 2970–2977.

666 Hansch, C., Leo, A., Hoekman, D., 1995. Exploring QSAR. Hydrophobic, electronic, and steric
667 constants. ACS Professional Reference Book. ACS, Washington.

668 Haynes, W.M. (Ed.), 2014. CRC Handbook of Chemistry and Physics, 95th Edition, CRC Handbook
669 of Chemistry and Physics, 95th Edition. CRC press.

670 Hwang, Y.S., Liu, J., Lenhart, J.J., Hadad, C.M., 2007. Surface Complexes of Phthalic Acid at the
671 Hematite/Water Interface. *J. Colloid Interface Sci.* 307 (1), 124–34.

672 Ilina, S.M., Maran, L., Lourino-Cabana, B., Eyrolle, F., Boyer, P., Coppin, F., Sivry, Y., Gélabert, A.,
673 Johnson, S.B., Yoon, T.H., Slowey, A.J., Brown, G.E., 2004. Adsorption of organic matter at
674 mineral/water interfaces: 3. Implications of surface dissolution for adsorption of oxalate. *Langmuir* 20,
675 11480–11492.

676 Kang, S., Xing, B., 2007. Adsorption of Dicarboxylic Acids by Clay Minerals as Examined by in Situ
677 ATR-FTIR and Ex Situ DRIFT. *Langmuir* 23 (13), 7024–31.

678 Karickhoff, S.W., Brown, D.S., Scott, T.A., 1979. Sorption of Hydrophobic Pollutants on Natural
679 Sediments. *Water Research* 13 (3), 241–48.

680 Karickhoff, S.W., 1981. Semi-empirical estimation of sorption of hydrophobic pollutants on natural
681 sediments and soils. *Chemosphere*, 10 (8), 833–846.

682 Karnitz, O., Gurgel, L.V.A., de Melo, J.C.P., Botaro, V.R., Melo, T.M.S., de Freitas Gil, R.P., Gil,
683 L.F., 2007. Adsorption of heavy metal ion from aqueous single metal solution by chemically modified
684 sugarcane bagasse. *Bioresour. Technol.* 98, 1291–1297.

685 Lerouge, C., Robinet, J.C., Debure, M., Tournassat, C., Bouchet, A., Fernández, A.M., Flehoc, C.,
686 Lerouge, C., Debure, M., Henry, B., Fernandez, A. M., Blessing, M., Proust, E., Madé, B., Robinet, J.
687 C. 2020. Origin of dissolved gas (CO₂, O₂, N₂, alkanes) in pore waters of a clay formation in the
688 critical zone (Tégulines Clay, France). *Appl. Geochem.* 104573.

689 Maes, N., Bruggeman, C., Govaerts, J., Martens, E., Salah, S., Van Gompel, M. 2011. A consistent
690 phenomenological model for natural organic matter linked migration of Tc(IV), Cm(III), Np(IV),
691 Pu(III/IV) and Pa(V) in the Boom Clay. *Phys. Chem. Earth* 36, 1590–1599.

692 Melkior, T., Yahiaoui, S., Thoby, D., Motellier, S., Barthès, V., 2007. Diffusion coefficients of
693 alkaline cations in Bure mudrock. *Phys. Chem. Earth* 32, 453–462.

694 Missana, T., Colàs, E., Grandia, F., Olmeda, J., Mingarro, M., García-Gutiérrez, M., Munier, I.,
695 Robinet, J.C., Grivé, M., 2017. Sorption of radium onto early cretaceous clays (Gault and Plicatules
696 Fm). Implications for a repository of low-level, long-lived radioactive waste. *Appl. Geochemistry* 86,
697 36–48.

698 Pageot, J., Rouzaud, J.N., Gosmain, L., Deldicque, D., Comte, J., Ammar, M.R., 2016. Nanostructural
699 characterizations of graphite waste from French gas-cooled nuclear reactors and links with ¹⁴C
700 inventory. *Carbon N. Y.* 105, 77–89.

701 Pageot, J., Rouzaud, J.N., Gosmain, L., Duhart-Barone, A., Comte, J., Deldicque, D., 2018. ¹⁴C
702 selective extraction from French graphite nuclear waste by CO₂ gasification. *Progress in Nuclear*
703 *Energy*, 105, 279–286.

704 Pignatello, J.J., Xing, B., 1996. Mechanisms of slow sorption of organic chemicals to natural particles.
705 *Environ. Sci. Technol.* 30 (1), 1–11.

706 Pinsuwan, S., Li, A., Yalkowsky, S.H., 1995. Correlation of Octanol/Water Solubility Ratios and
707 Partition Coefficients. *J. Chem. Eng. Data* 40, 623–626.

708 Poncet, B., Petit, L., 2013. Method to assess the radionuclide inventory of irradiated graphite waste
709 from gas-cooled reactors. *J. Radioanal. Nucl. Chem.* 298, 941–953.

710 Rasamimanana, S., Lefèvre, G., Dagnelie, R.V.H., 2017a. Adsorption of Polar Organic Molecules on
711 Sediments: Case-Study on Callovian-Oxfordian Claystone. *Chemosphere* 181, 296–303.

712 Rasamimanana, S., Lefèvre, G., Dagnelie, R.V.H., 2017b. Various Causes behind the Desorption
713 Hysteresis of Carboxylic Acids on Mudstones. *Chemosphere* 168, 559–67.

714 Sangster, J., 1989. Octanol-water partition coefficient of simple organic compounds. *J. Phys. Chem.*
715 *Ref. Data* 18 (3), 1111–1227.

716 Sarazin, G., Michard, G., Prevot F., 1999. A rapid and accurate spectroscopic method for alkalinity
717 measurements in sea water samples. *Water Res.* 33 (1), 290–294.

718 Savoye, S., Frasca, B., Grenut, B., Fayette, A., 2012. How mobile is iodide in the Callovo-Oxfordian
719 claystones under experimental conditions close to the in situ ones? *J. Contam. Hydrol.* 142–143, 82–
720 92.

721 Schaffer, M., Licha, T., 2015. A framework for assessing the retardation of organic molecules in
722 groundwater: Implications of the species distribution for the sorption-influenced transport. *Sci. Total*
723 *Environ.* 524–525, 187–194.

724 Shackelford, C.D., Moore, S.M., 2013. Fickian diffusion of radionuclides for engineered containment
725 barriers: Diffusion coefficients, Porosities, And complicating issues. *Eng. Geol.* 152, 133–147.

726 Tournassat, C., Gaboreau, S., Robinet, J.-C., Bourg, I.C., Steefel, C.I., 2016. Impact of microstructure
727 on anion exclusion in compacted clay media. *The Clay Minerals Society Workshop Lectures Series*,
728 21 (11), 137–149.

729 Vinsot, A., Anthony, C., Appelo, J., Lundy, M., Wechner, S., Cailteau-Fischbach, C., de Donato, P.,
730 Pironon, J., Lettry, Y., Lerouge, C., De Cannière, P. 2017. Natural Gas Extraction and Artificial Gas
731 Injection Experiments in Opalinus Clay, Mont Terri Rock Laboratory (Switzerland). *Swiss Journal of*
732 *Geosciences* 110 (1), 375–90.

733 Wersin, P., Soler, J.M., Van Loon, L., Eikenberg, J., Baeyens, B., Grolimund, D., Gimmi, T.,
734 Dewonck, S., 2008. Diffusion of HTO, Br⁻, I⁻, Cs⁺, 85Sr²⁺ and 60Co²⁺ in a clay formation: Results
735 and modelling from an in situ experiment in Opalinus Clay. *Applied Geochem.* 23, 4, 678-691.

736 Wigger, C., Gimmi, T., Muller, A., Van Loon, LR. 2018. The Influence of Small Pores on the Anion
737 Transport Properties of Natural Argillaceous Rocks – A Pore Size Distribution Investigation of
738 Opalinus Clay and Helvetic Marl. *Appl. Clay Sci.* 156, 134–143.

739 Willemsen, J.A.R., Myneni, S.C.B., Bourg, I.C. 2019. Molecular dynamics simulations of the
740 adsorption of phthalate esters on smectite clay surfaces. *J. Phys. Chem. C*, 123, 13624-13636.

Graphical Abstract

